

# A Point Light Source Interference Removal Method for Image Dehazing

Yanyang Yan<sup>1</sup>, Shengdong Zhang<sup>2</sup>, Mingye Ju<sup>3</sup>, Wenqi Ren<sup>1</sup>, Rui Wang<sup>1</sup>, and Yuanfang Guo<sup>4\*</sup>

<sup>1</sup>SKLOIS, IIE, CAS <sup>2</sup>Wuhan University <sup>3</sup>Nanjing University of Posts and Telecommunications  
<sup>4</sup>School of Computer Science and Engineering, Beihang University

## Abstract

Single image haze removal has been a challenging problem and the performance of the most existing dehazing methods is degraded when point light sources exist in the hazy image. In this paper, we propose a point light source interference removal method (PLiSIR) to reduce the interferences when estimating the atmospheric light. According to our observation, the pixel intensity around the point light sources can be modeled approximately by Gaussian distribution. The locations of the interfered pixels are obtained reasonably regardless of the specific number of light sources. A binary masking map is then created for distinguishing whether the pixel is affected by light sources and thus PLiSIR can be adopted to dehazing algorithms by removing the interfered pixels, during the estimation of the atmospheric light. To demonstrate how to apply PLiSIR to different algorithms, we select the dark channel prior dehazing method (DCP) and the color attenuation prior dehazing method (CAP) as two carrier methods and introduce the adaptations accordingly. Experimental results indicate that the PLiSIR can assist DCP and CAP to better estimate the atmospheric light, and thus generate better dehazing results compared to the original DCP and CAP methods. Moreover, PLiSIR also helps DCP and CAP to simplify the parameter adjustment process of the guided filter. At last, we compare our modified DCP approach (which we refer to PLiSIR-DCP) with the state-of-the-art nighttime dehazing algorithm to present an approach which is suitable for both daytime and nighttime haze removal.

## 1. Introduction

Many computer vision applications [12, 11, 13, 15, 34, 35], such as image retrieval, image classification, object tracking, etc., benefits from input images with decent quality and suffers from degraded ones. Currently, images captured at outdoor may be deteriorated (causing color decay, lower contrast, higher noise) by bad weathers like haze, rains and

etc. Therefore, numerous dehazing techniques [2, 8, 6, 22, 31, 32] are proposed to reduce the deterioration caused by haze and restore clear scenes. It not only increases the visual quality of the obtained images, but also provide input images with better quality to the latter applications.

The major challenge when developing haze removal techniques is that the concentration of the haze is dependent on the unknown depth in the hazy image. Initially, researchers apply traditional image enhancement tools, such as histogram equalization [28], to the hazy image for haze removal. However, this approach may cause color shifting of the scene since the contrast of the image is increased. Later, different researchers try to improve the dehazing performance via different mechanisms, such as polarization-based methods in [20, 16] and haze removal with known depth information [19, 7].

He *et al.* propose the dark channel prior (DCP) in [4]. Although DCP presents decent dehazing results in many cases, it fails to provide good results when there exist point light sources in the scene. This failure is caused due to the overestimation of the atmospheric light when the point light sources exist. Also, DCP possesses high complexity due to the adaptation of soft matting [9] and cannot process sky images properly. After DCP [4] proposed, numerous approaches [3, 30] are proposed to reduce the computational load. Since the algorithms based on DCP will estimate the atmospheric light by some maximum value selecting criteria in the hazy image or a local neighborhood, these DCP based methods still suffer from light interferences when there exist point light sources.

In 2015, Zhu *et al.* propose a novel color attenuation prior (CAP) [39] and create a linear model for the scene depth of the hazy image with supervised learning. Then the scene depth and thus the transmission map and the atmospheric light can be estimated, and the single image dehazing can be carried out. Still, CAP obtains worse atmospheric light estimation results when point light sources exist, and thus the final dehazing results.

The above mentioned approaches are designed for daytime hazy images. Recently, researchers also started to investigate the nighttime haze removal problem. In 2012, Pei

\*corresponding author

*et al.* in [21] map the colors of a nighttime haze image to those of a daytime haze image with a color transfer technique, which causes unrealistic colors in the dehazed results. Later, Zhang *et al.* propose a dehazing system in [36] which includes spatially varying light estimation and compensation, color correction and dehazing steps. However, the glow effect appears on the dehazed images generated by [36]. To reduce the glow effect, Li *et al.* [14] introduce a nighttime haze model which consists of direct transmission, the haze, and the glow estimations. Although they successfully solved the glow effect, the dehazed image shows unreal point light sources and some flat regions reveal obvious noise. In general, these nighttime haze removal methods generate unsatisfactory results when processing daytime hazy images.

In addition to priors-based dehazing methods, there are also many deep learning based approaches to solve the image enhancement problem [26, 33], including image dehazing [25, 27, 37, 38], in recent years. Cai *et al.* [1] propose an end-to-end convolutional neural network (CNN) to estimate the transmission map. Ren *et al.* proposed a multi-scale deep model to estimate the transmission map. Li *et al.* [10] reformulate the atmospheric model and design an AOD-Net to learn the mapping function between the hazy input and the corresponding clean image. Ren *et al.* [23, 24] use multi-scale networks fusion-based strategy to estimate the transmission map or directly restore a clear image from a hazy image. However, all these CNN-based networks cannot remove haze from nighttime scenes with point light sources.

In summary, when the hazy image contains some point light sources, the above-mentioned dehazing methods probably encounter a problem that the pixels interfered by the point light sources can easily be regarded as the most haze-opaque region, leading to an overestimated atmospheric light and sometimes a problematic estimated transmission map.

To reduce the point light source interferences, this paper contributes as follows.

- We observe that the existing dehazing algorithms usually perform worse when there exist point light sources in the hazy image due to the inaccurate estimation of the atmospheric light.
- We propose a point light source interference removal method (PLiSIR), which can be easily applied to the different dehazing algorithms such as DCP and CAP, to reduce the point light source interferences.
- Experimental results demonstrate that PLiSIR can assist DCP and CAP to obtain a better estimation of the atmospheric light and the depth map, respectively, and the modified DCP (PLiSIR-DCP) and modified CAP (PLiSIR-CAP) can generate better dehazing results compared to the original DCP and CAP methods. Moreover, PLiSIR also helps DCP and CAP to simplify

the parameter adjustment process of the guided filter where the dynamic ranges of suitable parameters are extended.

- We also compare the PLiSIR-DCP approach with the state-of-the-art nighttime haze removal algorithm [14] to present an approach which is suitable for both daytime and nighttime haze removal.

The remainder of this paper is organized as follows: In Sec. 2, we review the mainstream atmospheric scattering model, one popular haze removal algorithm (DCP) in [5] and one latest algorithm (CAP) in [39] respectively. Sec. 3 presents the proposed method and two examples of applying it to the carrier algorithms (applied to DCP and CAP). The experimental results are given in Section 4 and Section 5 concludes the paper.

## 2. Backgrounds

In this section, the mainstream atmospheric scattering model adopted in recent years will be introduced at first. Then, two haze removal algorithm, DCP and CAP, which will be exploited as the carrier algorithm later in the experiments, will be briefed accordingly.

### 2.1. Atmospheric Scattering Model

In recent years, the most widely adopted atmospheric scattering model is proposed in [18],[17],[29]. The model is defined as Eq. 1 shows.

$$\mathbf{I}(x) = \mathbf{J}(x)t(x) + \mathbf{A}(1 - t(x)) \quad (1)$$

where  $x$  is the position of the pixel,  $\mathbf{I}$  represents the hazy image,  $\mathbf{J}$  stand for the scene radiance (the haze-free image),  $\mathbf{A}$  represents the atmospheric light and  $t$  is the transmission ratio which indicates the portion of real scenes being captured by the camera. Note that  $\mathbf{I}$ ,  $\mathbf{J}$  and  $\mathbf{A}$  are all three-dimensional vectors in R-G-B space. When the atmosphere is homogeneous, the transmission  $t$  can be expressed as Eq. 2 shows.

$$t(x) = e^{-\beta * d(x)} \quad (2)$$

where  $\beta$  is the atmosphere scattering coefficient and  $d$  is the depth of the scene.

As we can conclude from Eq. 1, to recover the real scene  $\mathbf{J}$ ,  $\mathbf{A}$  and  $t$  must be estimated first.

### 2.2. Dark Channel Prior

In 2009, by performing numerous experiments on outdoor haze-free images, He *et al.* discover that in most of the natural scene patches, at least one of the color channels possesses some pixels with close to zero intensities. Then they propose the popular dark channel prior (DCP) in [5] as Eq. 3 shows.

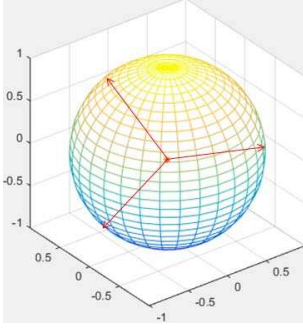


Figure 1. Light spreading model of a point light source.

$$J^{\text{dark}} = \min_{y \in \Omega(x)} \left( \min_{c \in r, g, b} J^c(y) \right) \quad (3)$$

where  $J^c$  is a color channel of  $\mathbf{J}$  and  $\Omega(x)$  represents a local patch centered at  $x$ . Once the atmospheric light  $\mathbf{A}$  is given, Eq. 1 can be normalized to

$$\frac{I^c(x)}{A^c} = t(x) \frac{J^c(x)}{A^c} + 1 - t(x) \quad (4)$$

To calculate the transmission map, the atmospheric light  $\mathbf{A}$  will be estimated first. He *et al.* simply obtain the location of the brightest pixel in the dark channel map  $J^{\text{dark}}$  and employ the co-located pixel value in  $\mathbf{I}$  as  $\mathbf{A}$ . Later, for better robustness, He *et al.* also exploit to obtain the locations of the top 0.1 percent brightest pixels in  $J^{\text{dark}}$  and then calculate the average value of the co-located pixel values in  $\mathbf{I}$  as  $\mathbf{A}$ . Once  $\mathbf{A}$  is estimated, the transmission map  $t$  can be calculated. After the atmospheric light and the transmission map obtained, the scene radiance can be recovered by Eq. 5.

$$\mathbf{J}(x) = \frac{\mathbf{I}(x) - \mathbf{A}}{t} + \mathbf{A} \quad (5)$$

### 2.3. Color Attenuation Prior

Eq. 2 indicates that the scene transmission  $t$  is attenuated exponentially with the depth  $d$ . Thus, Zhu *et al.* propose to first recover  $t$  via depth estimation in [39] and then calculate the atmospheric light and the scene radiance. Based on experiments, the concentration of the haze is found to be correlated with the differences between the brightness channel and the saturation channel in the Hue, Saturation, Value (HSV) color model. Then they propose a linear model as Eq. 6 shows.

$$d(x) = \theta_0 + \theta_1 v(x) + \theta_2 s(x) + \epsilon(x), \quad (6)$$

where  $x$  still represents the pixel index,  $d$  still represents the the depth,  $v$  is the brightness component,  $s$  is the saturation component,  $\theta_0, \theta_1, \theta_2$  are unknown linear coefficients and  $\epsilon(x)$  is a gaussian random variable with zero mean to represent the random error.

With the depth map, the transmission can be calculated via Eq. 2. As for the atmospheric light estimation, they search the location of the brightest pixel in the depth map  $d$ , and employ the co-located pixel value in the haze image  $\mathbf{I}$  as  $\mathbf{A}$ . At last, the scene radiance  $\mathbf{J}$  can be recovered according to Eq. 5.

### 3. Methodology

When the existing dehazing methods estimate the atmospheric light during the dehazing process, they may encounter a problem when the picture contains point light sources. Since the point light sources usually increase the values of neighboring pixels, they may overestimate the atmospheric light and thus the dehazing performance decreases. Therefore, we propose a point light source interferences removal method called PLSIR to increase the estimation accuracy.

To remove the interferences of point light sources, the light interfering range and locations of the point light sources must be found. At first, we introduce the case of a single point light source. In reality, a point light source affects a sphere-like three-dimensional neighborhood as Fig. 1 shows. The total light intensity from a light source is a constant which won't be changed by the distance between the current sphere surface and the point light source itself. Since the surface area is directly proportional to the squared radius of the sphere, the average light intensity on the surface is inversely proportional to the squared radius. Once the radius is known, the average light intensity can be easily calculated. As the radius increases, the average light intensity decreases. When a certain threshold is achieved, the light interferences to the objects on the current distance can be neglected. When locating a point light source and its light interfering range on a single image, it is of great challenge to get an accurate depth map and transform the two-dimensional depth map to the three-dimensional true distance map.

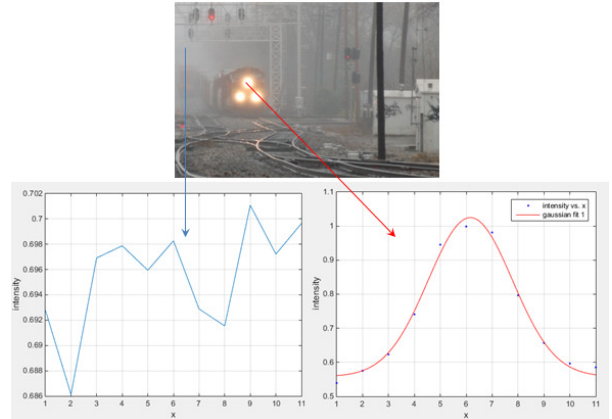


Figure 2. Distributions of pixel intensities.

Although it is hard to rebuild a three dimensional scene

Table 1. Relationship between the retained area and cut-off parameters .

interval	area proportion
$(\mu-\sigma, \mu+\sigma)$	0.683
$(\mu-1.96*\sigma, \mu+1.96*\sigma)$	0.954
$(\mu-2.58*\sigma, \mu+2.58*\sigma)$	0.997

model based on a single image, we can still locate the point light source and its light interfering range. During the experiments, we observe that the distribution of the pixel intensities around a point light source can be approximately modeled by Gaussian distribution as Fig. 2 shows, while the pixel intensities of unaffected pixels reveal a random distribution. Then the point light source and its light interfering range can be located by fitting the observed the pixel intensity distribution to Gaussian distribution. The expression of Gaussian distribution is in Eq. 7,

$$f(x) = \frac{1}{\sqrt{2\pi}\sigma} \exp\left(-\frac{(x-\mu)^2}{2\sigma^2}\right) \quad (7)$$

where  $\mu$  is the mean value and  $\sigma$  is the variance of  $f(x)$ . These two parameters both influence the shape of distribution.

During the curve fitting process, the location of the point light source can simply be selected as the location of the mean value  $\mu$ . Besides, as we can conclude from Tab. 1, the area between the curve and the  $x$  axis are related to  $\mu$  and  $\sigma$ . So when the difference between  $x$  and  $\mu$  exceeds a threshold  $T_d$ , we consider the Gaussian distribution is close to zero, i.e., the pixels farther than the threshold distance  $T_d$  is considered to be unaffected by the point light source. Refer to Tab. 1,  $T_d = 2.5 * \sigma$  is selected throughout the rest of this paper.

For each hazy image, a binary masking map  $\mathbf{M}$  is created to indicate whether the current pixel is interfered by the point light source. After the curve fitting process, suppose the index of each pixel is  $(i,j)$ , the masking map  $\mathbf{M}$  is defined in Eq. 8. Each value in  $\mathbf{M}$  is set to be zero initially.

$$\mathbf{M}_{(i,j)} = \begin{cases} 1 & \text{pixel}(i,j) \text{ is affected} \\ 0 & \text{pixel}(i,j) \text{ is unaffected} \end{cases} \quad (8)$$

For a given hazy image, our method is always feasible despite the image contains a point light source or not. Generally, pixels close to a point light source possess higher intensity than those faraway. The closer to the light source, the brighter a pixel should be. In the input image, we simply locate the pixel with largest intensity and assume it is a point light source. Then we select nearby pixels and proceed the curve fitting to fit the selected samples' distribution to Gaussian distribution. Since in a two dimensional image, the distances between horizontal nearby pixels are more close to the real distances in three dimensional reality, we choose the

nearby pixels in the horizontal direction. For convenience, we set the threshold distance  $T_d$  as a constant regardless of the direction.

Considering that using the distribution of one pixel's intensity may lead to inaccurate result, the distribution of the average intensity of pixel blocks is explored to improve the robustness. Experiments indicate a certain improvement compared to pixel based distributions. As mentioned before, pixel intensity around the light source is approximately Gaussian distributed while the others are not, then the curve fitting effectiveness can be applied to judge whether a point light source exists in the hazy image. Here, we choose the sum of square error, R-squared, root mean square error and adjusted R-squared as the discrimination criteria for the fitting effectiveness. In the curve fitting process, various block sizes are tested to obtain the best size according to these discrimination criteria.

If the curve fitting process fails to provide a decent fitting result, we consider there is no point light source in the hazy image, because the pixel with the largest intensity usually lies in the farthest region with random distributed intensities in that region when no point light source exists in the hazy image. For these hazy images, we considered as no point light source, we simply make no modifications to the masking map, i.e., the hazy image can still be dehazed by the carrier dehazing method.

Once fitting well, the parameters of the Gaussian distribution can be obtained accordingly. The average  $\mu$  represents a more accurate location of the point light source. The pixels, whose distance to the light source is less than  $T_d$ , are regarded as light interfered pixels and the masking map is modified according to Eq. 8.

In reality, an image usually contains multiple point light sources. Then, our previous method to locate the single point light source and its interference range needs to be revised to adapt. In PLiSIR, we first carry out the previous single point light source algorithm to obtain an initial masking map. Then we sort pixels from large intensity to small. According to the orders, one pixel is selected in every iteration. If its corresponding value in  $\mathbf{M}$  is 1, the current pixel is already being classified as a light interfered pixel and we proceed to the next iteration. Otherwise, we assume the current location exists a point light source and carry out the previous curve fitting method to further identify the existence of the point light source and its potential affecting area. After the masking map is updated accordingly, the algorithm then proceeds to the next iteration. The iteration process is terminated when the pixel intensity is smaller than a threshold  $T_f$ . To adapt different image content,  $T_f$  is set as a variable proportional to the largest pixel intensity in the image.

A final masking map  $\mathbf{M}$  can be obtained after iterations, i.e. the light interfered areas are identified at last. Fig. 3 presents three examples of applying our method to hazy im-

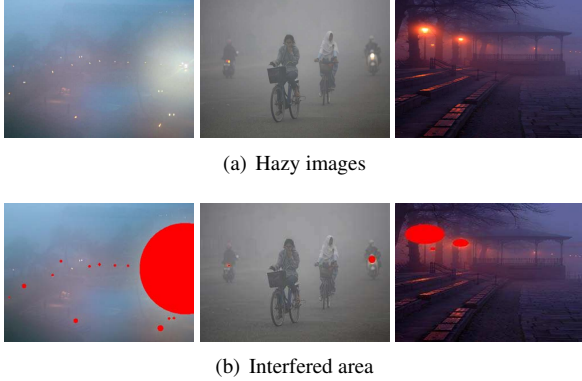


Figure 3. Results of interfered area detection.

ages with multiple point light sources. As can be observed, the majority of the point light source interferences are identified and located except for those tiny ones. According to our experiments, these unidentified tiny light sources do not degrade the final dehazing results in most of the cases.

Once the final masking map  $M$  is obtained, it can be adopted to different carrier dehazing algorithms to reduce the point light source interferences when estimating the atmospheric light. To demonstrate the adaptation of PLSiSIR to the carrier algorithms, DCP and CAP will be employed as the carriers in this paper, as they represent the most popular and latest methods. The modified DCP and CAP algorithm will be represented by PLSiSIR-DCP and PLSiSIR-CAP respectively.

In PLSiSIR-DCP, the majority steps are identical to the original DCP except for the selection of the locations of potential values for the atmospheric light. During that process, by referring to  $M$ , we select the top 0.1 percent brightest pixels with no point light source interferences in the dark channel image.

In PLSiSIR-CAP, our approach is adopted during the step of estimating the atmospheric light from the depth map. According to the masking map  $M$ , PLSiSIR-CAP selects the top 0.1 percent largest pixels with no point light source interferences in the depth map as the potential atmospheric light locations.

## 4. Experimental Results

Since our approach is suitable for various haze removal algorithms, we apply PLSiSIR to the popular algorithm He *et al.*'s DCP algorithm [5] and the latest Zhu *et al.*'s CAP algorithm [39] and compare to the original methods respectively. Based on the fact that the two carrier algorithms have different theoretical systems and haze removal mechanisms, experimental results demonstrate the importance of PLSiSIR regardless of the carrier algorithm. At last, since the existing nighttime dehazing methods [36] and [14] have the ability to process the nighttime hazy images with point light sources, we compare the current the latest nighttime dehazing method

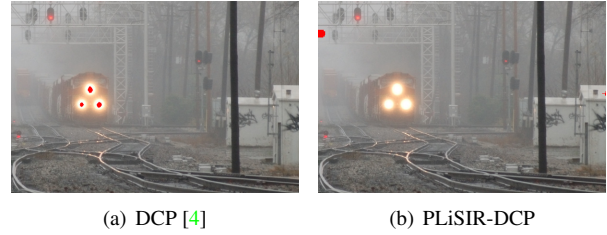


Figure 4. Comparison of the selected pixels for atmospheric light estimation.

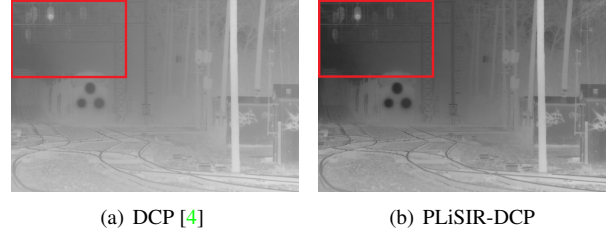


Figure 5. Results of estimated transmission maps.

Table 2. Estimation of atmospheric light.

Picture	DCP estimated A	PLSiSIR-DCP A
Fig. 7(a)	(0.897,0.905,0.901)	(0.586,0.594,0.609)
Fig. 7(d)	(0.999,1.000,0.998)	(0.750,0.751,0.754)

[14], whose results are favorable among the existing nighttime dehazing methods, with PLSiSIR employing DCP as the carrier.

### 4.1. Experiments with Dark Channel Prior

In the DCP algorithm [5], the transmission map  $t$  is calculated according to the estimated atmospheric light  $A$  and then being refined by the guided filter. Thus, it is of great importance to obtain an accurate  $A$  when calculating  $t$ . In the experiments, the haze images are processed with the original DCP and the modified algorithm PLSiSIR-DCP. Fig. 4 shows the different atmospheric light selection of DCP and PLSiSIR-DCP. Tab. 2 shows the estimated atmospheric light of DCP and PLSiSIR-DCP. As can be observed, PLSiSIR-DCP select more reasonable locations for estimating the atmospheric light and generate more accurate atmospheric light value.

With a better estimated atmospheric light, better refined transmission map  $t$  is extracted during the dehazing process and the results are shown in Fig. 5. According to Fig. 5, we can conclude that the transmission map Fig. 5(b) generated by PLSiSIR-DCP possesses better contrast, i.e., it reveals the real depth of the scene more accurately compared to the original DCP, especially for the regions contains edges like tail and distant objects.

Guided filter has been widely adopted once proposed, because of its ability to reduce the halos and blocking artifacts. During the processing procedure, the final results are influ-

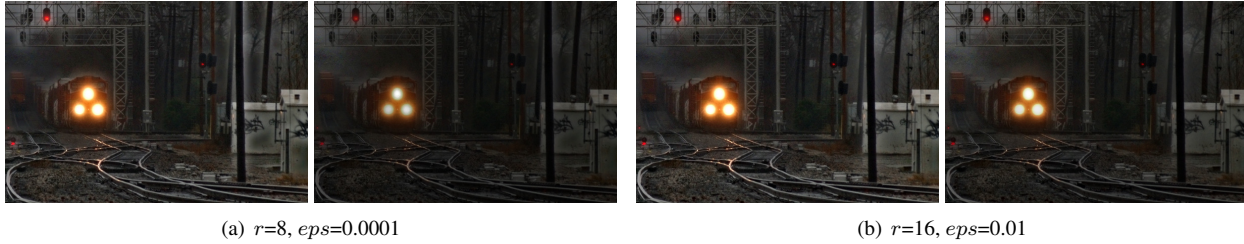


Figure 6. Results with unsuitable  $r$  and  $eps$ . For each pair, the left image is generated by DCP while the right one is generated by PLSIR-DCP.



Figure 7. Results with suitable parameters.

enced by two parameters, namely the local window radius  $r$  and the regularization parameter  $eps$ . Experimental results may vary greatly if one of them changes and the effect is being judged subjectively but not automatically, which leads to complicated parameter adjustment for good results. In reality, most algorithms just set specific parameters for all images to be processed for convenience. Although these specific parameters can lead to nearly satisfying results in many cases, they fails in some other cases. Fortunately, when remove the haze in images containing point light sources, PLSIR can effectively assist the parameter adjustment process of the guided filter. As is shown in Fig. 6, the quality about final refined dehazed images varies greatly with different parameters. Some refined dehazed images have high-quality while the others still have some halos or blocking artifacts. On the other hand, when applying PLSIR to DCP, the performance benefits from PLSIR and the interference of parameter adjustment decreases. As we can observe, some halos, which are obvious in images processed by the original algorithm with unsuitable guided filter parameters, become less noticeable when apply PLSIR-DCP with iden-

tical parameters to the same test image, which indicate that the proposed PLSIR can depress the halos and blocking artifacts. Thus with PLSIR, the cost of parameter adjustment can be reduced because the range of suitable parameters has been expanded and users can obtain reasonable final dehazing results more easily.

Fig. 7 shows some examples of guided filter results with suitable parameters. The halos and blocking artifacts can hardly be perceived. Except for the support to the parameter adjustment, our approach possesses other benefits as we can observe.

Firstly, the objects with small depth in the haze image have nearly no haze regardless of the parameter  $\beta$ , whose purpose is to add some reasonable haze such that the perceived scene  $J$  is closer to the reality. If the point light sources are ignored, these close objects may become too bright such that it looks like there still exist some haze, as the pavement shows in Fig. 7(h). Meanwhile, our modified algorithm generate better visual quality for those close objects. As for the distant objects in the scene, PLSIR-DCP gives much clearer results compared to DCP. As we can observe in Fig. 7, the trees in the left part of Fig. 7(c) shows some specific details while the details of corresponding trees in Fig. 7(b) is less visible. Moreover, for the faraway backgrounds, our dehazed images still maintains a rough outline while the original DCP generated images just gives haze-like scene, as Fig. 7(c) and 7(b) show. Therefore, PLSIR-DCP shows superior performance compared to DCP.

## 4.2. Experiments with Color Attenuation Prior

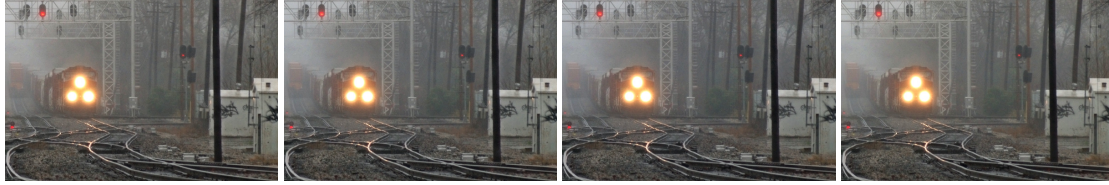
As mentioned in Section 2, the algorithm with the color attenuation prior [39] outperforms the previous haze removal algorithms in terms of both the dehazing effect and efficiency. Therefore, CAP is employed as another carrier of PLSIR.

Differernt from the DCP based algorithms, a scene depth is firstly computed in CAP based on a learned linear model. Once the scene depth map is calculated, the transmission map can be obtained according to Eq. 1 and the atmospheric light is also estimated from it.

In the experiments, PLSIR-CAP not only estimates the atmospheric light better, but also helps during the process



(a) CAP [39] with  $r=8,16,32,64$ ;  $eps=0.0001$



(b) Our proposed PLSIR-CAP with  $r=8,16,32,64$ ;  $eps=0.0001$



(c) CAP [39] with  $r=8,16,32,64$ ;  $eps=0.0001$



(d) Our proposed PLSIR-CAP with  $r=8,16,32,64$ ;  $eps=0.0001$

Figure 8. Results of various parameters.  $r=64$  gives best performance.

of parameter adjustment for the guided filter applied on the depth map, similar to PLSIR-DCP. As shown in Fig. 8, with identical parameters, PLSIR-CAP generates more natural dehazed images while the original CAP generates images with halos and blocking artifacts, especially at the edge regions such as the edges of telegraph pole. As we can observe, the more the parameters are unsuitable, the bigger difference is between PLSIR-CAP and CAP results. Also, PLSIR-CAP still outperforms CAP when comparing employing suitable parameters. Therefore, similar to PLSIR-DCP, we can conclude that PLSIR also helps CAP to depress the halos and blocking artifacts, which reduces the cost of parameter adjustment, and PLSIR-CAP gives better performance compared to CAP.

### 4.3. Comparisons to Nighttime Dehazing Algorithm

In this subsection, we compare PLSIR-DCP with the state-of-the-art nighttime haze removal algorithm [14] to illustrate that our PLSIR-DCP not only gives excellent performance for daytime haze removal, but also suitable for

nighttime haze removal.

Fig. 9 shows that [14] has its own merits and drawbacks. When dealing with distant area, [14] gives clearer result than PLSIR-DCP. For example, in the left image of Fig. 9(b), [14] generates clear bridge while PLSIR-DCP generates bridge surrounded by some haze. Still, our bridge is recovered compared to the hazy image and its railing can also be perceived if observe carefully. Meanwhile, some flat regions recovered by [14], like the sky, shows obvious noise and artifacts, which severely degrades the visual quality of the dehazed image. [14] also fails to recover the original shape of point light sources. Compared to [14], PLSIR-DCP's recovered images in Fig. 9 restores the point light sources much better. For example, PLSIR-DCP's street lamps region look more natural. Also, the noise and artifacts in some flat regions generated by [14] do not appear at the co-located regions of PLSIR-DCP's results. Moreover, PLSIR-DCP generated daytime dehazed images are much more natural compared to [14] generated results.



Figure 9. Comparisons between the proposed PLiSIR-DCP and the nighttime dehazing method of Li et al. [14].

## 5. Conclusion

This paper has focused on resolving an important problem, which most existing dehazing methods face, caused by point light source interferences. A point light source interference removal method (PLiSIR) is proposed to reduce the point light source interferences when estimating the atmospheric light. As demonstrated, PLiSIR can be applied to different dehazing algorithms such as DCP and CAP. In the experiments, PLiSIR shows excellent performance when assists DCP and CAP to estimate the atmospheric light and thus generate superior dehazing results compared to original DCP and CAP generated results. Also, PLiSIR helps the guided filter employed in DCP and CAP to simplify the parameter adjustment process. At last, the modified DCP approach (PLiSIR-DCP) is compared with the state-of-the-art nighttime dehazing algorithm to reveal its ability to perform both daytime and nighttime haze removal.

**Acknowledgments.** This work was supported in part by the National Natural Science Foundation of China under Grant 61802391 and 61802403, the Fundamental Research Funds for Central Universities, the CCF-Tencent Open Fund, and Zhejiang Lab’s International Talent Fund for Young Professionals.

## References

- [1] Bolun Cai, Xiangmin Xu, Kui Jia, Chunmei Qing, and Dacheng Tao. Dehazenet: An end-to-end system for single image haze removal. *TIP*, 25(11):5187–5198, 2016. 2
- [2] R. Fattal. Single image dehazing. *ACM Trans. Graphics*, 27(3):–, 2008. 1
- [3] K.B. Gibson, D.T. Vo, and T.Q. Nguyen. An investigation of dehazing effects on image and video coding. *IEEE Trans. Image Process.*, 12(2):662–673, 2012. 1
- [4] K. He, J. Sun, and X. Tang. Single image haze removal using dark channel prior. In *CVPR*, pages 1956–1963, 2009. 1, 5, 6
- [5] K. He, J. Sun, and X. Tang. Single image haze removal using dark channel prior. *IEEE Trans. Pattern Anal. Mach. Intell.*, 33(12):2341–2353, 2011. 2, 5
- [6] L. Kratz K. Nishino and S. Lombardi. Bayesian defogging. *Int. J. Comput. Vis.*, 98(3):263–278, 2012. 1
- [7] J. Kopf. Deep photo: Model-based photograph enhancement and viewing. *ACM Trans. Graphics*, 27(5), 2008. 1
- [8] L. Kratz and K. Nishino. Factorizing scene albedo and depth from a single foggy image. in *Proc. IEEE Int. Conf. Comput. Vis.*, pages 1701–1708, 2009. 1
- [9] A. Levin, D. Lischinski, and Y. Weiss. A closed-form solution to natural image matting. *IEEE Trans. Pattern Anal. Mach. Intell.*, 30(2):228–242, 2008. 1
- [10] Boyi Li, Xiulian Peng, Zhangyang Wang, Jizheng Xu, and Dan Feng. An all-in-one network for dehazing and beyond. In *ICCV*, 2017. 2

- [11] Boyi Li, Wenqi Ren, Dengpan Fu, Dacheng Tao, Dan Feng, Wenjun Zeng, and Zhangyang Wang. Benchmarking single image dehazing and beyond. *TIP*, 2018. [1](#)
- [12] Chongyi Li, Chunle Guo, Wenqi Ren, Runmin Cong, Junhui Hou, Sam Kwong, and Dacheng Tao. An underwater image enhancement benchmark dataset and beyond. *TIP*, 2020. [1](#)
- [13] Siyuan Li, Iago Breno Araujo, Wenqi Ren, Zhangyang Wang, Eric K Tokuda, Roberto Hirata Junior, Roberto Cesar-Junior, Jiawan Zhang, Xiaojie Guo, and Xiaochun Cao. Single image deraining: A comprehensive benchmark analysis. In *CVPR*, 2019. [1](#)
- [14] Y. Li, R. Tan, and M.S. Brown. Nighttime haze removal with glow and multiple light colors. in *Proc. IEEE Int. Conf. Comput. Vis.*, 2015. [2](#), [5](#), [7](#), [8](#)
- [15] Yu Liu, Guanlong Zhao, Boyuan Gong, Yang Li, Ritu Raj, Niraj Goel, Satya Kesav, Sandeep Gottimukkala, Zhangyang Wang, Wenqi Ren, et al. Improved techniques for learning to dehaze and beyond: A collective study. *arXiv preprint arXiv:1807.00202*, 2018. [1](#)
- [16] S.G. Narasimhan and S.K. Nayar. Chromatic framework for vision in bad weather. in *Proc. IEEE Conf. Comput. Vis. Pattern Recognit.*, pages 598–605, 2000. [1](#)
- [17] S.G. Narasimhan and S.K. Nayar. Chromatic framework for vision in bad weather. in *Proc. IEEE Conf. Comput. Vis. Pattern Recognit.*, 1:598–605, 2000. [2](#)
- [18] S.G. Narasimhan and S.K. Nayar. Vision and the atmosphere. *Int. J. Comput. Vis.*, 48:233–254, 2002. [2](#)
- [19] S.G. Narasimhan and S.K. Nayar. Interactive (de) weathering of an image using physical models. in *Proc. IEEE Workshop Color Photometric Methods Comput. Vis.*, 6, 2003. [1](#)
- [20] S.K. Nayar and S.G. Narasimhan. Vision in bad weather. in *Proc. IEEE Int. Conf. Comput. Vis.*, 2:820–827, 1999. [1](#)
- [21] S.C. Pei and T.Y. Lee. Nighttime haze removal using color transfer pre-processing and dark channel prior. in *Procs. IEEE Int. Conf. Image Process.*, pages 957–960, 2012. [2](#)
- [22] Wenqi Ren and Xiaochun Cao. Deep video dehazing. In *Pacific rim conference on multimedia*, 2017. [1](#)
- [23] Wenqi Ren, Si Liu, Hua Zhang, Jinshan Pan, Xiaochun Cao, and Ming-Hsuan Yang. Single image dehazing via multi-scale convolutional neural networks. In *ECCV*, 2016. [2](#)
- [24] Wenqi Ren, Lin Ma, Jiawei Zhang, Jinshan Pan, Xiaochun Cao, Wei Liu, and Ming-Hsuan Yang. Gated fusion network for single image dehazing. In *CVPR*, 2018. [2](#)
- [25] Wenqi Ren, Jinshan Pan, Hua Zhang, Xiaochun Cao, and Ming-Hsuan Yang. Single image dehazing via multi-scale convolutional neural networks with holistic edges. *International Journal of Computer Vision*, pages 1–20, 2019. [2](#)
- [26] Wenqi Ren, Jiaolong Yang, Senyou Deng, David Wipf, Xiaochun Cao, and Xin Tong. Face video deblurring using 3d facial priors. In *ICCV*, 2019. [2](#)
- [27] Wenqi Ren, Jingang Zhang, Xiangyu Xu, Lin Ma, Xiaochun Cao, Gaofeng Meng, and Wei Liu. Deep video dehazing with semantic segmentation. *TIP*, 28(4):1895–1908, 2018. [2](#)
- [28] J.A. Stark. Adaptive image contrast enhancement using generalizations of histogram equalization. *IEEE Trans. Image Process.*, 9(5):889–896, 2000. [1](#)
- [29] R.T. Tan. Visibility in bad weather from a single image. in *Proc. IEEE Conf. Comput. Vis. Pattern Recognit.*, pages 1–8, 2008. [2](#)
- [30] K. Tang, J. Yang, and J. Wang. Investigating haze-relevant features in a learning framework for image dehazing. in *Procs. IEEE Conf. Comput. Vis. Pattern Recognit.*, pages 2995–3002, 2014. [1](#)
- [31] Qingbo Wu, Wenqi Ren, and Xiaochun Cao. Learning interleaved cascade of shrinkage fields for joint image dehazing and denoising. *TIP*, 29:1788–1801, 2019. [1](#)
- [32] Qingbo Wu, Jingang Zhang, Wenqi Ren, Wangmeng Zuo, and Xiaochun Cao. Accurate transmission estimation for removing haze and noise from a single image. *TIP*, 2019. [1](#)
- [33] Yanyang Yan, Wenqi Ren, and Xiaochun Cao. Recolored image detection via a deep discriminative model. *TIFS*, 14(1):5–17, 2018. [2](#)
- [34] Wenhan Yang, Ye Yuan, Wenqi Ren, Jiaying Liu, Walter J Scheirer, Zhangyang Wang, et al. Advancing image understanding in poor visibility environments: A collective benchmark study. *TIP*, 2020. [1](#)
- [35] Ye Yuan, Wenhan Yang, Wenqi Ren, Jiaying Liu, Walter J Scheirer, and Zhangyang Wang. Ug2+ track 2: A collective benchmark effort for evaluating and advancing image understanding in poor visibility environments. *arXiv preprint arXiv:1904.04474*, 2019. [1](#)
- [36] J. Zhang, Y. Cao, and Z. Wang. Nighttime haze removal based on a new imaging model. in *Procs. IEEE Int. Conf. Image Process.*, pages 4557–4561, 2014. [2](#), [5](#)
- [37] Shengdong Zhang, Fazhi He, Wenqi Ren, and Jian Yao. Joint learning of image detail and transmission map for single image dehazing. *The Visual Computer*, pages 1–12, 2018. [2](#)
- [38] Shengdong Zhang, Wenqi Ren, and Jian Yao. Feed-net: Fully end-to-end dehazing. In *ICME*, 2018. [2](#)
- [39] Q. Zhu, J. Mai, and L. Shao. A fast single image haze removal algorithm using color attenuation prior. *IEEE Trans. Image Process.*, 24(11), 2015. [1](#), [2](#), [3](#), [5](#), [6](#), [7](#)